Reprinted from:
ADVANCES IN ATOMIC AND
MOLECULAR PHYSICS, VOL. 8

MONTE CARLO TRAJECTORY CALCULATIONS OF ATOMIC AND MOLECULAR EXCITATION IN THERMAL SYSTEMS

JAMES C. KECK

Department of Mechanical Engineering
Massachusetts Institute of Technology
Cambridge, Massachusetts

I. Introduction

Within the framework of classical mechanics Monte Carlo trajectory calculations (Wall *et al.*, 1961) provide an exact method for investigating reactions in atomic and molecular systems. They constitute, in effect, numerical experiments in which the equations of motion for a system are integrated using digital or analog computers to determine the course of the reactions for prescribed sets of initial conditions. The results of the experiments can be recorded and used to calculate cross sections and rate constants in exactly the same manner as in real experiments.

To carry out a Monte Carlo calculation for a given atomic or molecular system one needs to know the interaction potential for the system. Although in principle this can be obtained from quantum mechanics, reliable potential functions are only available for a few relatively simple systems, and it is usually necessary to assume a parametric form for the interaction. In cases such as $H^+ + e + e$ or $H + H + H$, where the interaction potential is

known, the comparison between Monte Carlo calculations and the corresponding experimental results provides a critical test of the validity of the classical approximation for the system under investigation. In most other cases, particularly those involving heavy particles, the uncertainty resulting from the use of classical mechanics is small compared to that introduced by assuming the interaction potential; a comparison of Monte Carlo and experimental results provides a method for determining the potential parameters.

Numerous investigations of atomic and molecular collisions have been made using Monte Carlo methods. [References to this literature can be found in recent papers by Morokuma and Karplus (1971), Mok and Polanyi (1970), Kuntz *et al.* (1970), and Bunker and Pattengill (1968).] Most of these have involved unimolecular decay or bimolecular exchange reactions of the type

$$AB \longrightarrow A + B \tag{1}$$

and

$$AB + C \longrightarrow A + BC \tag{2}$$

where the particles A, B, and C have been either ions, atoms, or molecules. By contrast, relatively few applications of the method to excitation or dissociation reactions of type

$$AB + C \longrightarrow AB^* + C \tag{3}$$

and

$$AB + C \longrightarrow A + B + C \tag{4}$$

have been reported (Keck, 1962; Woznick, 1965a; Mansbach and Keck, 1969; Abrines *et al.*, 1966; Abrines and Percival, 1966). The reason for this is undoubtedly due in part to the fact that the usual impact parameter sampling technique employed in the calculations for exchange reactions is extremely inefficient when applied to excitation reactions.

To circumvent this difficulty the author has developed an "inside out" sampling technique based on the variational theory (Keck, 1967) of reaction rates. This technique involves selection of initial conditions inside the collision complex, followed by integration of the equations of motion both forward and backward in time to obtain the complete history of a collision. The most important advantage of sampling inside the collision complex is that the reaction probability for excitation and dissociation can be increased sufficiently to make Monte Carlo calculations for these processes relatively efficient.

The purpose of this article is to present a systematic discussion of Monte Carlo methods for studying thermal excitation and dissociation in atomic and molecular systems and to review the results that have been obtained. In the following section we shall consider first the description of thermal

excitation and dissociation processes by means of master equations and equivalent diffusion equations. This will be followed by a discussion of Monte Carlo techniques for obtaining the transition kernels and transport coefficients required for solution of these equations. Finally we shall discuss the numerical results that have been obtained for molecular and atomic systems.

II. Master Equation

In this paper we are concerned with three-body excitation and dissociation reactions of the type shown in Eqs. (3) and (4). We assume that the interaction potential is known and that the motion of the particles can be described using classical mechanics. We further assume that the translational and rotational degrees of freedom have a Boltzmann distribution. Under these conditions it has been shown by Keck and Carrier (1965) that the relaxation of the molecules AB may be described by a master equation of the form

$$N_e(\varepsilon)\frac{\partial X(\varepsilon, t)}{\partial t} = \int_{-\delta}^{0} R(\varepsilon', \varepsilon)[X(\varepsilon', t) - X(\varepsilon, t)]\, d\varepsilon' + R(c, \varepsilon)[X(\infty, t) - X(\varepsilon, t)] \tag{5}$$

where t is the time, $\varepsilon = (E - B)/kT$ is the energy relative to the top of the rotational barrier in units of kT, $\delta = D/kT$ is the dissociation energy in units of kT, $N_e(\varepsilon)\, d\varepsilon$ is the equilibrium concentration of molecules in the range ε to $\varepsilon + d\varepsilon$,

$$X(\varepsilon, t) = N(\varepsilon, t)/N_e(\varepsilon) \tag{6}$$

is the ratio of concentration of molecules at ε to the corresponding equilibrium concentration,

$$X(\infty, t) = [\mathrm{A}][\mathrm{B}]/[\mathrm{A}]_e[\mathrm{B}]_e \tag{7}$$

is the ratio of the product of the concentrations of A and B to the corresponding product at equilibrium, $R(\varepsilon', \varepsilon)\, d\varepsilon'\, d\varepsilon$ is the equilibrium rate of transitions from $d\varepsilon$ to $d\varepsilon'$, and

$$R(c, \varepsilon) = \int_0^{\infty} R(\varepsilon', \varepsilon)\, d\varepsilon' \tag{8}$$

is the equilibrium rate of transitions from $d\varepsilon$ to the dissociated state.

Note that by definition

$$R(\varepsilon', \varepsilon) = K(\varepsilon', \varepsilon)N_e(\varepsilon) = K(\varepsilon, \varepsilon')N_e(\varepsilon') = R(\varepsilon, \varepsilon') \tag{9}$$

and

$$R(c, \varepsilon) = K(c, \varepsilon)N_e(\varepsilon) = K(\varepsilon, c)[\mathrm{A}]_e[\mathrm{B}]_e = R(\varepsilon, c) \tag{10}$$

where K is the usual transition rate constant and we have assumed detailed balancing.

As may be inferred from the work of Montroll and Shuler (1958) and Brau, Keck, and Carrier (1966), the evolution of a system described by (5) from any initial distribution to final equilibrium begins with a rapid relaxation to a quasisteady distribution which is "almost Boltzmann" over most of the range $-\delta < \varepsilon < 0$. This initial phase, during which dissociation and recombination are negligible, has a duration of the order of the vibrational relaxation time and, except at very high temperatures, is followed by a much longer phase during which most of the dissociation and recombination occurs and the "almost Boltzmann" distribution is maintained in a quasisteady state. During this latter phase the left-hand side of (5) is very small for all energies greater than $(-\delta + 1)$ and may be set equal to zero. Under these conditions the "almost Boltzmann" distribution can be closely approximated by the form

$$X(\varepsilon, t) = \begin{cases} X(\infty, t) + [X(-\delta, t) - X(\infty, t)]\chi(\varepsilon); & \varepsilon < 0 \\ X(\infty, t) & \varepsilon > 0 \end{cases} \tag{11}$$

where $\chi(-\delta) \equiv 1$ and $\chi(\varepsilon)$ is a solution of the steady state master equation

$$0 = \int_{-\delta}^{0} R(\varepsilon', \varepsilon)[\chi(\varepsilon') - \chi(\varepsilon)]\, d\varepsilon' - R(c, \varepsilon)\chi(\varepsilon). \tag{12}$$

Substituting (11) into (5) and integrating both sides from $-\delta$ to 0 we find

$$\partial[\mathrm{AB}]/\partial t = [X(\infty, t) - X(-\delta, t)]R_{\mathrm{N}} \tag{13}$$

where

$$R_{\mathrm{N}} = \int_{-\delta}^{0} R(c, \varepsilon)\chi(\varepsilon)\, d\varepsilon = \int_{-\delta}^{0}\int_{0}^{\infty} R(\varepsilon'\varepsilon)\chi(\varepsilon)\, d\varepsilon'\, d\varepsilon \tag{14}$$

is the nonequilibrium steady state dissociation rate.

In the temperature range where the steady state approximation is valid $N_{\mathrm{e}}(\varepsilon)$ has a strong maximum at $\varepsilon = -\delta$, and it is a good approximation to set

$$[\mathrm{AB}] = \int_{-\delta}^{0} X(\varepsilon, t)N_{\mathrm{e}}(\varepsilon)\, d\varepsilon \approx X(-\delta, t)[\mathrm{AB}]_{\mathrm{e}}. \tag{15}$$

Introducing (15) and (7) into (13) we obtain the familiar phenomenological rate equation

$$\partial[\mathrm{AB}]/\partial t = k_{\mathrm{r}}[\mathrm{A}][\mathrm{B}][\mathrm{C}] - k_{\mathrm{d}}[\mathrm{AB}][\mathrm{C}], \tag{16}$$

where the steady state recombination and dissociation rate constants k_{r} and k_{d} are defined by

$$k_{\mathrm{r}}[\mathrm{A}]_{\mathrm{e}}[\mathrm{B}]_{\mathrm{e}}[\mathrm{C}] = k_{\mathrm{d}}[\mathrm{AB}]_{\mathrm{e}}[\mathrm{C}] = R_{\mathrm{N}}. \tag{17}$$

The corresponding equilibrium rate constants k_{re} and k_{de} are defined by

$$k_{re}[A]_e[B]_e[C] = k_{de}[AB]_e[C] = R(0), \tag{18}$$

where

$$R(0) = \int_{-\delta}^{0} R(c, \varepsilon)\, d\varepsilon = \int_{-\delta}^{0} \int_{0}^{\infty} R(\varepsilon'\varepsilon)\, d\varepsilon'\, d\varepsilon \tag{19}$$

is the "one way" equilibrium dissociation rate. As will be seen later, $\chi(\varepsilon) \leq 1$, so that (17) and (18) imply

$$k_d/k_r = k_{de}/k_{re} = [A]_e[B]_e/[AB]_e \tag{20}$$

and

$$k_d/k_{de} = k_r/k_{re} = R_N/R(0) \leq 1 \tag{21}$$

Thus, the steady rate constants k_r and k_d satisfy detailed balancing even though they are in general less than the corresponding equilibrium rate constants.

To evaluate the steady state rate constants using (14) and (17) we must find $\chi(\varepsilon)$ from the integral equation (12). There are several techniques for doing this, each of which is especially useful for kernels $R(\varepsilon', \varepsilon)$ of a particular character.

A. Solution by Iteration

If the energy transfer per collision associated with the transition kernel $R(\varepsilon', \varepsilon)$ is large compared to kT, it is relatively easy and efficient to solve (12) by iteration. To do this we simply rewrite the equation in the form

$$\chi^{(n+1)}(\varepsilon) = \int_{-\delta}^{0} R(\varepsilon', \varepsilon)\chi^{(n)}(\varepsilon')\, d\varepsilon'/Z(\varepsilon) \tag{22}$$

where

$$Z(\varepsilon) = \int_{-\delta}^{0} R(\varepsilon', \varepsilon)\, d\varepsilon' + R(c, \varepsilon) = \int_{-\delta}^{\infty} R(\varepsilon', \varepsilon)\, d\varepsilon' \tag{23}$$

is the equilibrium collision rate per unit ε and $\chi^{(n)}$ is the nth approximation to $\chi(\varepsilon)$. For strong coupling kernels of the type associated with statistical theories of reaction rates (e.g., see Keck and Kalelkar, 1968) a reasonable guess for $\chi^{(0)}(\varepsilon)$ will usually produce acceptable results in one or two iterations. In general, however, the transition kernels derived from Monte Carlo calculations imply energy transfer somewhat less than kT and in this case the solution of (12) by iteration is relatively inefficient.

B. Solution for a Separable Kernel

For a transition kernel which is separable in the form

$$R(\varepsilon', \varepsilon) = \begin{cases} r_1(\varepsilon) r_2(\varepsilon'); & \varepsilon < \varepsilon' \\ r_1(\varepsilon') r_2(\varepsilon); & \varepsilon' < \varepsilon \end{cases} \tag{24}$$

then, regardless of the energy transfer per collision, (12) may be transformed exactly into the equivalent diffusion equation (Keck and Carrier, 1965)

$$\frac{d}{d\varepsilon}\left(\frac{Z^2}{W}\right)\frac{d\chi}{d\varepsilon} = 0 \tag{25}$$

with the boundary condition

$$\left.\frac{d \ln \chi}{d\varepsilon}\right|_0 = -\left.\frac{r_+ W}{r_2 Z}\right|_0 \tag{26}$$

where

$$W(\varepsilon) = r_2(dr_1/d\varepsilon) - r_1(dr_2/d\varepsilon) \tag{27}$$

$$Z(\varepsilon) = r_2 r_- + r_1 r_+ \tag{28}$$

$$r_-(\varepsilon) = \int_{-\delta}^{\varepsilon} r_1(\varepsilon')\, d\varepsilon' \tag{29}$$

and

$$r_+(\varepsilon) = \int_{\varepsilon}^{\infty} r_2(\varepsilon')\, d\varepsilon'. \tag{30}$$

Integrating (25) and using (14) and (26) we obtain

$$\chi(\varepsilon) = 1 - R_N \int_{-\delta}^{\varepsilon} \left(\frac{W}{Z^2}\right) d\varepsilon' \tag{31}$$

where

$$\frac{R_N}{R(0)} = \left[1 + \int_{-\delta}^{0}\int_{-\delta}^{\varepsilon} R(c, \varepsilon)\left(\frac{W(\varepsilon')}{Z^2(\varepsilon')}\right) d\varepsilon'\, d\varepsilon\right]^{-1} \tag{32}$$

and we have assumed that $R(c, -\delta) \ll Z(-\delta)$, which is consistent with the use of the steady state approximation. This simply means that the fraction of molecules dissociating directly from energies within kT of the potential minimum is negligible. Comparing (32) and (21) we see that (32) is just the ratio k/k_e of the steady state and equilibrium rate constants.

C. Equivalent Diffusion Equation

If the energy transfer per collision associated with the kernel $R(\varepsilon', \varepsilon)$ is small compared to kT, the steady state master equation (32) may be con-

verted to the equivalent diffusion equation (Keck and Carrier, 1965)

$$\frac{d}{d\varepsilon}\left(\frac{\Delta_2}{2}\right)\frac{d\chi}{d\varepsilon} = 0 \tag{33}$$

where

$$\Delta_n(\varepsilon) = \int_{-\delta}^{0} (\varepsilon' - \varepsilon)^n R(\varepsilon', \varepsilon)\, d\varepsilon' \tag{34}$$

and we have used the approximation

$$\Delta_1 = \tfrac{1}{2}\, d\Delta_2/d\varepsilon \tag{35}$$

which is valid for kernels satisfying the condition

$$|(\partial R(\varepsilon', \varepsilon)/\partial\bar{\varepsilon})_\Delta| \ll |(\partial R(\varepsilon', \varepsilon)/\partial\Delta)_{\bar{\varepsilon}}| \tag{36}$$

where $\bar{\varepsilon} = (\varepsilon' + \varepsilon)/2$ is the mean of the initial and final energies, and $\Delta = (\varepsilon' - \varepsilon)$ is the energy transfer.

Integrating (33) and using the boundary condition

$$-\left(\frac{\Delta_2}{2}\right)\frac{d\chi}{d\varepsilon}\bigg| = \int_{-\delta}^{0} R(c, \varepsilon)\chi(\varepsilon)\, d\varepsilon \tag{37}$$

obtained by matching the diffusion flux to the dissociation rate, we find

$$\chi(\varepsilon) = 1 - R_N \int_{-\delta}^{\varepsilon} \left(\frac{2}{\Delta_2}\right) d\varepsilon' \tag{38}$$

where

$$\frac{R_N}{R(0)} = \left[1 + \int_{\delta}^{0}\int_{\delta}^{\varepsilon} R(c, \varepsilon)\left(\frac{2}{\Delta_2(\varepsilon')}\right) d\varepsilon'\, d\varepsilon\right]^{-1} \tag{39}$$

is the ratio (21) of the steady state and equilibrium rate constant in the diffusion approximation. In the limiting case of a separable kernel for which Z and W/Z^2 are slowly varying functions of ε, $\Delta_2/2$ approaches Z^2/W, and the results (39) of the diffusion approximation approach those (32) for the separable kernel.

This completes our discussion of the equations which may be used to describe the nonequilibrium dissociation and recombination process, and we now turn our attention to the problem of determining the required equilibrium transition kernel $R(\varepsilon', \varepsilon)$.

III. Transition Kernel

A. Variational Theory

To obtain a general expression for the transition kernel $R(\varepsilon', \varepsilon)$ suitable for evaluation by Monte Carlo methods, we start with the variational theory

(Keck, 1967) of reaction rates. We assume that the Hamiltonian $H(\mathbf{p}, \mathbf{q})$ of the system and the density of representative points in phase space $\rho(\mathbf{p}, \mathbf{q})$ are known and independent of the sign of $\mathbf{p}$. Then under steady state conditions the flux of points across a surface S dividing the initial and final states of the system is

$$R_V(S) = \int_{S(+)} \rho(\mathbf{v}\cdot\mathbf{n})\, dS = -\int_{S(-)} \rho(\mathbf{v}\cdot\mathbf{n})\, dS$$

$$= \frac{1}{2}\int_S \rho|\mathbf{v}\cdot\mathbf{n}|\, dS, \tag{40}$$

where $R_V(S)$ is the variational rate for the surface S, $\mathbf{v}$ is the generalized velocity, $\mathbf{n}$ is the unit normal to the surface element dS, and $S(+)$ and $S(-)$ denote the portions of the surface S on which $\mathbf{v}\cdot\mathbf{n}$ is positive and negative, respectively. If we further assume that the definition of S is independent of the sign of $\mathbf{p}$ and take into account the fact that a phase space trajectory connecting given initial (i) and final (f) states may cross S more than once, the transition rate from (i) to (f) may be expressed in the form

$$R(\mathrm{i}, \mathrm{f}) = \frac{1}{2}\int_S m^{-1} I(\mathrm{i}, \mathrm{f})\rho|\mathbf{v}\cdot\mathbf{n}|\, dS \tag{41}$$

where m is the number of times a trajectory crosses S and $I(\mathrm{i}, \mathrm{f}) = 1$ for trajectories passing through dS which connect i and f, and is zero otherwise.

To evaluate $R(\mathrm{i}, \mathrm{f})$ using a particular set of coordinates $(\mathbf{p}, \mathbf{q})$ we let $\phi(\mathbf{p}, \mathbf{q}) = 0$ be the equation of the surface S. Then the unit normal to dS is given by

$$\mathbf{n} = \nabla\phi/|\nabla\phi|, \tag{42}$$

and the element of length parallel to $\mathbf{n}$ is

$$dh = d\phi/|\nabla\phi| \tag{43}$$

where ∇ is the generalized gradient in phase space.

Using Hamilton's equation

$$\dot{p}_j = -\partial H/\partial q_j, \qquad \dot{q}_j = \partial H/\partial p_j \tag{44}$$

to obtain the components of $\mathbf{v}$ and observing that

$$dh\, dS = \prod_j dp_j\, dq_j \tag{45}$$

is just the volume element in phase space, the variational rate (40) can be written

$$R_V(S) = \frac{1}{2}\int_{\phi=0} \rho_V\, dH \prod_{j=2} dp_j\, dq_j \tag{46}$$

and the reaction kernel (41) can be written

$$R(\mathrm{i}, \mathrm{f}) = \frac{1}{2}\int_{\phi=0} m^{-1} I(\mathrm{i}, \mathrm{f}) \rho_V \, dH \prod_{j=2} dp_j \, dq_j, \tag{47}$$

where

$$\rho_V = \rho \left| 1 + \sum_{j=2} J\left(\frac{p_1 q_1}{p_j q_j}\right) \right| \tag{48}$$

is an effective density and

$$J\left(\frac{p_1 q_1}{p_j q_j}\right) = \frac{\partial p_1}{\partial p_j}\frac{\partial q_1}{\partial q_j} - \frac{\partial p_1}{\partial q_j}\frac{\partial q_1}{\partial p_j} \tag{49}$$

is the Jacobian of the transformation from $(p_1 q_1)$ to $(p_j q_j)$.

To determine the functions m and $I(\mathrm{i}, \mathrm{f})$ we must solve the equations of motion (44) for systems passing through S and, for three or more particles, this can only be done numerically. Under these conditions the transition kernel $R(\mathrm{i}, \mathrm{f})$ must also be evaluated numerically, and Monte Carlo methods are ideally suited to the problem. They enable one not only to integrate the equations of motion, but simultaneously to evaluate the multidimensional integrals in (46) and (47).

B. Monte Carlo Method

A general discussion of Monte Carlo methods may be found in the literature (Hammersley and Handscomb, 1964; Meyer, 1956). In the present application we are concerned with the evaluation of multidimensional integrals of the form

$$R = \int f(\mathbf{x}) \, d\mathbf{x} \tag{50}$$

where $\mathbf{x}$ denotes a point in an n-dimensional space, $d\mathbf{x}$ is the volume element and $f(\mathbf{x})$ is a positive definite function whose value can only be determined after the value of $\mathbf{x}$ has been specified. We wish to estimate the value of R by random sampling of the integrand in the domain of $\mathbf{x}$. Let $w(\mathbf{x})$ be the density of sample points in the vicinity of $\mathbf{x}$. We require that $w(\mathbf{x})$ be easily integrable and normalized so that

$$\int w(\mathbf{x}) \, d\mathbf{x} = 1 \tag{51}$$

We next divide the domain of integration into finite regions Δ_i sufficiently small so that the variation of $w(\mathbf{x})$ in Δ_i is negligible but sufficiently large to

contain a reasonable number of sample points. The integral (50) can then be approximated in the form

$$R = \sum_i \left(\frac{\Delta_i}{n_i}\right) \sum_j^{n_i} f_j \tag{52}$$

where

$$n_i = w_i \Delta_i N \tag{53}$$

is the number of sample points in Δ_i, N is the total number of sample points, w_i is the mean value of $w(x)$ for Δ_i, and f_j is the value of $f(\mathbf{x})$ at the sample point $\mathbf{x}_j$ in Δ_i. Substituting (53) into (52) and observing that $w_i \approx w_j$ for all points in Δ_i, we obtain

$$R = \frac{1}{N} \sum_i \sum_j^{n_i} \left(\frac{f_j}{w_j}\right) = \frac{1}{N} \sum_j^{N} \left(\frac{f_j}{w_j}\right) \tag{54}$$

where the sum in the last expression for R is taken over all sample points in the domain of integration. Note that $w(\mathbf{x})$ must be positive unless $f(\mathbf{x}) \equiv 0$.

To obtain a set of sample points distributed in accord with $w(\mathbf{x})$ we introduce the conditional probability distribution functions

$$P_k(x_1 \cdots x_{k-1} | \alpha_k) = (W_{k-1})^{-1} \int_{-\infty}^{\alpha_k} W_k \, dx_k \tag{55}$$

where

$$W_k(x_1 \cdots x_k) = \int_{-\infty}^{\infty} dx_{k+1} \cdots \int_{-\infty}^{\infty} dx_n \, w(\mathbf{x}) \tag{56}$$

is the probability density for the first k coordinates of $\mathbf{x}$. We then generate a sequence of random numbers $Y_1 \cdots Y_n$ uniformly distributed on the interval 0 to 1 (Meyer, 1956). Using these numbers, the coordinates $\alpha_1 \cdots \alpha_n$ of a sample point can be determined by solving the set of equations

$$P_k = Y_k; \qquad 1 \leq k \leq n \tag{57}$$

in ascending order. This procedure may be repeated to produce as many points as desired. If the density function is separable as a product in the form

$$w(\mathbf{x}) = \prod_i^n w_i(x_i) \tag{58}$$

then the distribution functions (55) become

$$P_k(\alpha_k) = \left[\int_{-\infty}^{\infty} w_k(x) \, dx\right]^{-1} \int_{-\infty}^{\alpha_k} w_k(x) \, dx \tag{59}$$

and the coordinates may be chosen independently. This result can easily be generalized to situations in which $w(\mathbf{x})$ can be separated as a product in any form.

In most previous applications of Monte Carlo methods to reaction rates, the distribution of sample points has been specified arbitrarily as a matter of convenience. This is rarely the best procedure and it is usually possible to improve the efficiency of the calculations considerably by optimizing the distribution function. To do this we assume that the values f_j of the unknown function $f(\mathbf{x})$ at the various sample points $\mathbf{x}_j$ can be treated as independent random variables. Using (52) the expectation value of R can then be written

$$\langle R \rangle = \sum_i \Delta_i \langle f \rangle_i \tag{60}$$

where we have assumed that the expectation value of f_j is the same for all points in the volume element Δ_i. For the same set of assumptions the variance of R

$$\sigma^2(R) = \langle (R - \langle R \rangle)^2 \rangle = \langle R^2 \rangle - \langle R \rangle^2 \tag{61}$$

is easily shown to be

$$\sigma^2(R) = n_i^{-1} \sum_i \Delta_i^2 \sigma_i^2(f) \tag{62}$$

Minimizing the fractional error $\sigma/\langle R \rangle$ for a fixed number of sample points

$$N = \sum_i n_i \tag{63}$$

we obtain the optimum density of sample points

$$w_{i0} = n_i/\Delta_i N = \sigma_i(f) \left[\sum_j \Delta_j \sigma_j(f) \right]^{-1} \tag{64}$$

or in integral form

$$w_0(\mathbf{x}) = \sigma(f) \left[\int \sigma(f)\, d\mathbf{x} \right]^{-1} \tag{65}$$

In deriving this expression we have tacitly ignored the additional constraint that $w(\mathbf{x})$ be integrable analytically. It is clear, however, that we should choose our integrable $w(\mathbf{x})$ to approximate $w_0(\mathbf{x})$ as closely as possible.

Using (64) to eliminate Δ_i in (62), we obtain the expression

$$\sigma(R) = N^{-1/2} \sum_i \Delta_i \sigma_i(f) \tag{66}$$

or

$$\sigma(R) = N^{-1/2} \int \sigma(f)\, d\mathbf{x} \tag{67}$$

for the standard deviation of R associated with the optimum distribution.

For the case of the rate integral (47), the integrand in (50) has the form

$$f(\mathbf{x}) = m^{-1} I(\mathrm{i}, \mathrm{f}) \rho_V \tag{68}$$

and its Monte Carlo approximation (54) can be written

$$R(\mathrm{i}, \mathrm{f}) = \frac{1}{N} \sum_j^N \left(\frac{I(\mathrm{i}, \mathrm{f}) \rho_V}{mw} \right)_j . \tag{69}$$

The optimum density of points obtained from (65) is

$$w_0(\mathbf{x}) = \rho_V \sigma(m^{-1} I) \left[\int \rho_V \sigma(m^{-1} I)\, d\mathbf{x} \right]^{-1} \tag{70}$$

To evaluate $\sigma(m^{-1}I)$ we let $p_m(\mathbf{x})$ be the probability that a trajectory sampled on the surface S connects i to f with m crossings of S, then

$$\sigma^2(m^{-1} I) = \sum_m \frac{p_m}{m^2} - \left(\sum_m \frac{p_m}{m} \right)^2 . \tag{71}$$

For the special case in which $p_m = 0$ for $m > 1$, we obtain the familiar result

$$\sigma(m^{-1} I) = [p_1 (1 - p_1)]^{1/2} \tag{72}$$

associated with the binomial distribution.

In general $p_m(\mathbf{x})$ is unknown or can only be roughly estimated *a priori*, and it is necessary to assume its form initially. As the calculations proceed, however, the distribution can be systematically improved by using the accumulated results to approximate $p_m(\mathbf{x})$ in a given region Δ_j using the relation

$$p_{mj} \approx f_{mj} , \tag{73}$$

where f_{mj} is the fraction of points sampled in Δ_j which cross the sample surface S,m times during the reaction. In the important special case where $p_m(\mathbf{x})$ is independent of the position of the point in the sample surface, (70) reduces to

$$w_V(\mathbf{x}) = \rho_V / R_V(S) \tag{74}$$

Substituting this expression for w in (69) we find

$$R(\mathrm{i}, \mathrm{f}) = R_V(S) N^{-1} \sum_j^N [m^{-1} I(\mathrm{i}, \mathrm{f})]_j . \tag{75}$$

If, as is usually the case, ρ_V is not readily integrable but we can find a reasonably close approximation ρ_A which is, then (69) also gives

$$R(\mathrm{i}, \mathrm{f}) = \frac{R_A}{N} \sum_j^N \left[\frac{I(\mathrm{i}, \mathrm{f}) \rho_V}{m \rho_A} \right]_j , \tag{76}$$

where

$$R_A = \int \rho_A \, dH \prod_j dp_j \, dq_j \tag{77}$$

and we have set

$$w_A(\mathbf{x}) = \rho_A / R_A . \tag{78}$$

The approximation for ρ_A must of course satisfy the requirement $\rho_A > 0$ unless $\rho_V \equiv 0$.

C. Initial Conditions

The efficiency of Monte Carlo calculation is influenced not only by the manner in which points are sampled on a given surface, but also by the choice of surface. In most Monte Carlo studies (Morokuma and Karplus, 1971; Mok and Polanyi, 1970; Kuntz *et al.*, 1970; Bunker and Pattengill, 1968; Abrines *et al.*, 1966; Abrines and Percival, 1966) the points have been sampled on what may be called the "impact parameter surfaces." For two particles with a relative separation $\mathbf{r}$ these surfaces may be defined by the equation

$$(\mathbf{r} \cdot \dot{\mathbf{r}})/|\dot{\mathbf{r}}| = a \tag{79}$$

where a is the "stand-off" distance which must be greater than the range of the interaction potential between the particles. The variational rate (46) for the "impact parameter surfaces" is

$$R_V(IP) = \int \rho |\dot{\mathbf{r}}| 2\pi b \, db \, d\mathbf{p} \, d\mathbf{P} \, d\mathbf{R} \tag{80}$$

where $b = |\mathbf{r} \times \dot{\mathbf{r}}|/|\dot{\mathbf{r}}|$ is the impact parameter, $\mathbf{p}$ is the relative momentum, and $\mathbf{P}$ and $\mathbf{R}$ are the momentum and position of the center of mass. As is well known, this rate diverges and convergence of the corresponding transition kernel $R(\mathrm{i}, \mathrm{f})$ depends on the fact that the transition probability $\langle m^{-1} I(\mathrm{i}, \mathrm{f}) \rangle$ goes to zero for large values of b. In sampling on the "impact parameter surfaces" the divergence of $R_V(IP)$ is usually handled by cutting off the impact parameter b at some maximum value b_m. This cut-off must be chosen with some care, however. If it is too large the fraction of reacting trajectories may be very small and the calculations become very inefficient. If it is too small some reacting trajectories may be omitted and an artificial bias is introduced into the results. The principal advantage of the "impact parameter surfaces" is that they permit *a priori* specification of the phase space density in the initial state. This is important if one wishes to simulate the results of beam experiments carried out for particles in precisely defined states. If any appreciable averaging is involved or if results are required for a sequence of initial conditions this advantage rapidly disappears.

For the simulation of reaction rates under thermal conditions it is usually far more efficient to sample on surfaces passing through the collision complex and to integrate the equations of motion forward and backward in

time to the initial and final states. This not only materially increases the fraction of "reacting" trajectories but also permits one to terminate the integration of the equations of motion as soon as it becomes clear that the interaction has become negligible, a condition easier to recognize going out of a collision than into it. One has a great deal of freedom when sampling is carried out in the collision complex and the best choice of surface depends on the class of reactions being studied. In this connection the variational theory (Keck, 1967) can be of considerable assistance.

To our knowledge the only Monte Carlo calculations that have been reported using sample surfaces interior to the collision complex are those carried out by the author and his co-workers on excitation and dissociation in three-body collisions (Keck, 1962; Woznick, 1965a; Mansbach and Keck, 1969). The surfaces used in this work were defined by the conditions.

$$E - B = E_0 \leq 0; \qquad r \leq z \tag{81}$$

where E_0 is the energy of the surface with respect to the top of the rotational barrier, z is the radius of the rotational barrier, and r is the separation of the atoms forming the molecule. The variational rate $R_V(E_0)$ for the "barrier surfaces" has been evaluated by Woznick (Keck, 1967) for Morse potentials and Mansbach and Keck (1969) for Coulomb potentials. The expressions are somewhat complicated and will not be given here as they are not required for our present purposes. For Morse potentials the "barrier rates" are finite and give a rigorous upper bound to the true rates which are, in general, within a factor of 10 of the experimentally observed rates. For Coulomb potentials the "barrier rate" diverges linearly with the distance of the "third body" from the center of mass of the atom and a cut-off must be introduced. Even so, the divergence is one order lower than that for the "impact parameter surfaces," and it was this which made Monte Carlo calculations of atomic excitation and ionization under thermal conditions feasible.

IV. Molecular Excitation and Dissociation

Using the methods discussed above Keck (1962) and Woznick (1965a) have investigated the excitation and dissociation of simple diatomic molecules in three-body collisions. Attention was focused on states within a few kT of the dissociation limit since it was anticipated that these would be most important for determining the steady state dissociation and recombination rate constants. Furthermore, this is the region in which classical mechanics should be a good approximation due to the high density of states and large quantum mechanical transition probabilities involved.

Most of the calculations were for homonuclear molecules interacting with purely repulsive third bodies; however, a few recent results for heteronuclear molecules interacting with repulsive third bodies and homonuclear molecules interacting with third bodies characterized by potentials with a weakly attracting minimum are also included (Shui, private communication). It was assumed that superposition applied so that the full three-body potential could be represented by a sum of pairwise interactions in the form

$$V = V_{12}(r_{12}) + V_{23}(r_{23}) + V_{13}(r_{13}) \tag{82}$$

where the molecular interaction $V_{12}(r_{12})$ was always of the Morse form

$$V_M(r) = D_e(1 - e^{-\beta_e(r-r_e)})^2 \tag{83}$$

and the interactions with the third body $V_{13}(r_{13})$ and $V_{23}(r_{23})$ were of the Morse form for the attracting cases and of the exponential form

$$V_E(r) = Ae^{-r/L} \tag{84}$$

for the repulsive cases. The potential parameters used are summarized in Table I. As will be seen the results were surprisingly insensitive to these parameters.

TABLE I

POTENTIAL PARAMETERS

	Morse				Exponential	
	D_e(eV)	$\beta_e(A^{-1})$	$r_e(A)$		A(eV)	L(Å)
H_2	4.75	1.93	.74	HeH	134	0.27
N_2	9.90	2.69	1.10	HeCl	547	0.27
O_2	5.18	2.65	1.21	HeI	790	0.29
Cl_2	2.51	2.03	1.99	ArH	268	0.35
I_2	1.57	1.86	2.67	ArO	760	0.35
HCl	4.62	1.87	1.28	ArCl	1060	0.35
NAr	.017	1.49	3.18	ArI	1510	0.39
ClAr	.033	1.41	3.39	XeO	915	0.40

The trajectories were sampled on that portion of the "barrier surfaces" (81) where $\mathbf{v}\cdot\mathbf{n} < 0$ using the weight function (74). Although this function is not as easy to integrate as one might wish, the possibility of using simpler approximate forms and correcting in the manner of (76) was overlooked in the initial work. A detailed discussion of the "barrier surfaces" and associated crossing rates $R_V(E_0)$ is given by Keck (1967).

The six coupled equations of motion (44) for the relative motion of the three particles were integrated using standard fourth-order Runge–Kutta and predictor-corrector methods on IBM 7090 and 360-65 computers.

Tolerances were set by requiring energy conservation to within .01 kT and angular momentum conservation to within 0.1%. To determine a complete trajectory the equations of motion were integrated both forward and backward in time until the interaction potential fell below .01 kT and the third body was moving outward.

A few typical trajectories illustrating the various reactions which can occur are shown in Figs. 1 and 2. The cases presented, H_2 + Ar at $kT/D = 0.01$

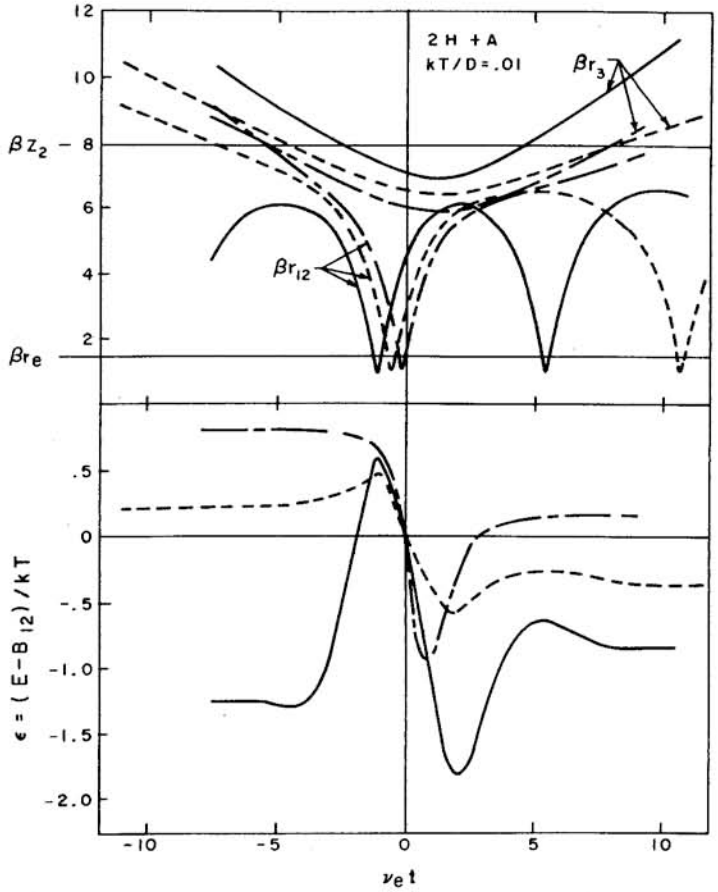

FIG. 1. Typical trajectory histories for H_2 + Ar collisions at $kT/D = .01$. Shown plotted in dimensionless form are the separation r_{12} of the H atoms, the distance r_3 of the Ar from the center of mass of H_2 and the energy relative to the top of the rotational barrier $(E - B)$. $\nu_e = 1.3 \times 10^{14}$ sec^{-1} is the ground state vibrational frequency of H_2, $\beta = 1.93 \times 10^8$ cm^{-1} is the range parameter for the Morse potential, r_e is the equilibrium separation, and z_2 is the most probable position of the rotational barrier.

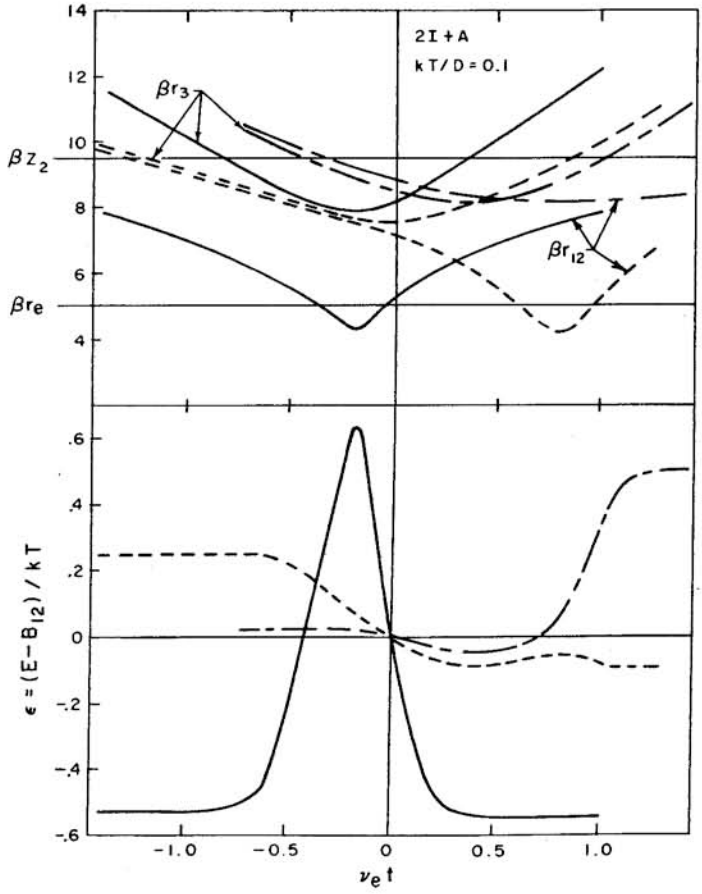

FIG. 2. Typical trajectory histories for $I_2 + Ar$ collisions at $kT/D = 0.1$. $\nu_e = 6.5 \times 10^{12}$ sec^{-1} is the ground state vibrational frequency of I_2 and $\beta = 1.86 \times 10^8$ cm^{-1} is the range parameter for the Morse potential. Other quantities are defined in the caption of Fig. 1.

and $I_2 + Ar$ at 0.1, are two extremes in the ratio of collision time to the vibrational period of the molecule. Examples of free–bound (fb), free–free (ff), and bound–bound (bb) transitions, are shown. These figures enable one to observe the general character of the particle trajectories and energy exchanges for molecules crossing the surface $\varepsilon = (E - B)/kT = 0$. The molecular vibrations are highly anharmonic and the energy exchanges are typically of order kT or less.

Table II shows the distribution of trajectories with respect to the number of crossings of the surface $\varepsilon = 0$ in the free–bound direction for several

TABLE II

DISTRIBUTION OF TRAJECTORIES WITH RESPECT TO CLASS OF REACTION AND NUMBER OF TRAVERSALS k OF THE TRIAL SURFACE IN FREE BOUND DIRECTION[a]

Class	θ	$k=1$	2	3	Total
A. $2\,H + A$					
$N(f\|k\|b)$	.01	94	28	0	122
	.1	60	26	3	89
$N(f\|k\|f)$	.01	74	8	2	84
	.1	91	19	0	110
$N(b\|k\|b)$	.01	119	14	2	135
	.1	108	16	1	125
$N(b\|k\|f)$	.01	19	1	0	20
	.1	26	2	0	28
$N(dE/dT>0)$[b]	.01	35	4	0	39
	.1	36	11	1	48
Total	.01	341	55	4	400
	.1	321	74	5	400
B. $2\,O + A$					
$N(f\|k\|b)$	.01	146	33	2	181
	.1	128	31	0	159
$N(f\|k\|f)$	.01	81	4	0	85
	.1	77	14	0	91
$N(b\|k\|b)$	.01	94	8	0	102
	.1	100	6	0	106
$N(b\|k\|f)$	.01	15	0	0	15
	.1	13	1	0	14
$N(dE/dt>0)$[b]	.01	12	5	0	17
	.1	28	2	0	30
Total	.01	348	50	2	400
	.1	346	54	0	400
C. $2\,I + A$					
$N(f\|k\|b)$	.01	256	7	0	263
	.1	282	4	0	286
$N(f\|k\|f)$	.01	48	0	0	48
	.1	44	0	0	44
$N(b\|k\|b)$	.01	69	1	0	70
	.1	39	1	0	40
$N(b\|k\|f)$	.01	0	0	0	0
	.1	5	0	0	5
$N(dE/dt>0)$[b]	.01	16	3	0	19
	.1	25	0	0	25
Total	.01	389	11	0	400
	.1	395	5	0	400

systems at $kT/D = 0.01$ and 0.1. It can be seen that the number of multiple crossings decreases as the ratio of the mass of the molecule to the mass of the third body increases, i.e., as the collisions become more impulsive. Using this data, the net fraction of "reacting" trajectories can be obtained from (68) and is given by

$$\frac{R(0)}{R_V(0)} = \frac{1}{N_0(0)} \sum_j^{N_0} \left[\frac{I(0)}{k}\right]_j = \frac{N(0)}{N_0(0)} \tag{85}$$

where $N_0(0)$ is the number of sample points, $k = (m + 1)/2$ is the number of times a trajectory crosses the surface $\varepsilon = 0$ in the free–bound direction, and $I(0) = 1$ if $\varepsilon_i > 0 > \varepsilon_f$, and is zero otherwise. The values of this fraction for all of the systems studied are given in Table III. Also given are the number of points sampled, the masses m_1 and m_3 of the recombining atoms and third bodies, and the two parameters $[m_3/(m_1 + m_3)]^{1/2}$ and βL. In the case of HCl, m_1 was taken to be the mass of H since the variational rate for collisions with the Cl end of the molecule is negligible. The systems are arranged in order of increasing $[m_3/(m_1 + m_3)]^{1/2}$, and it can be seen that a strong correlation exists. This is shown graphically in Fig. 3 and may be represented by the empirical equation

$$N(0)/N_0(0) = 1 - 0.7[m_3/(m_1 + m_3)]^{1/2}. \tag{86}$$

A correlation of this type is reasonable, since as $m_3 \to 0$, the collisions become impulsive and recrossings do not occur, while for $m_3 \to \infty$, the net energy transfer to the third body tends to zero and recrossing is highly probable. The exact form of the correlation is not understood, however. Based on this correlation, which applies strictly only to homonuclear and highly asymmetric heteronuclear molecules interacting with third bodies that are in all cases effectively repulsive, we suggest the expression

$$\frac{N(0)}{N_0(0)} = 1 - 0.7\left[\frac{m_2}{m_1 + m_2}\left(\frac{m_3}{m_1 + m_3}\right)^{1/2} + \frac{m_1}{m_1 + m_2}\left(\frac{m_3}{m_2 + m_3}\right)^{1/2}\right] \tag{87}$$

as a reasonable approximation for a general diatomic molecule interacting with a repulsive third body. No other statistically significant correlation either with kT/D or βL has been found. This is somewhat surprising and suggests that the transitions occur primarily as a result of a "spectator

---

FOOTNOTES TO TABLE II:

[a] The parameter $\theta = kT/D$.

[b] These trajectories which crossed the trial surface in the wrong direction arose from an approximation made in separating the weighting function (74) in which only nearest neighbor interactions were taken into account. They were eliminated in compiling the statistical results.

TABLE III

REACTING FRACTIONS $N(0)/N_0(0)$ FOR SURFACE $E - B = 0$

	m_1	m_3	$\left(\frac{m_3}{m_1+m_3}\right)^{1/2}$	βL	$\frac{kT}{D}$	$N_0(0)$	$\frac{N(0)}{N_0(0)}$
$I_2 + He$	127	4	.175	.54	0.1	200	$.87 \pm .03$
					.01	200	$.80 \pm .03$
$O_2 + Ar^a$	16	1	.24	.93	0.1	25	$.90 \pm .06$
					.01	25	$.78 \pm .08$
$O_2{}^a + Ar$	400	40	.30	.93	0.1	25	$.76 \pm .09$
					.01	25	$.76 \pm .09$
$I_2 + Ar$	127	40	.49	.72	0.1	800	$.70 \pm .02$
					.01	400	$.67 \pm .03$
$Cl_2 + Ar$	35	40	.73	.72	.05	600	$.56 \pm .02$
$O_2 + Ar$	16	40	.85	.93	0.1	800	$.39 \pm .02$
					.01	800	$.41 \pm .02$
$N_2 + Ar$	14	40	.86	.90	0.1	300	$.38 \pm .03$
					.01	300	$.50 \pm .03$
$HCl + He$	1	4	.89	.51	0.1	300	$.41 \pm .03$
$O_2 + Xe$	16	131	.94	1.06	0.1	800	$.37 \pm .02$
					.01	400	$.34 \pm .03$
$H_2 + Ar$	1	40	.99	.68	0.1	400	$.21 \pm .02$
					.01	400	$.30 \pm .03$
$HCl + Ar$	1	40	.99	.65	0.1	300	$.25 \pm .03$
					.05	300	$.34 \pm .03$

[a] Fictional species having masses indicated but correct force constants.

process" in which the third body collides with one end of the molecule and there is negligible momentum transfer to the other.

To obtain information about the transition rates between bound molecular states, calculations for trajectories sampled on the surfaces $\varepsilon = -1, -2$, and -3 were also made. From them one can construct the transition kernel $R(\varepsilon_i, \varepsilon_f)$ for states near the dissociation limit using the approximation based on (75)

$$R(\varepsilon_i, \varepsilon_f) = \frac{R_V(\varepsilon)}{N_0(\varepsilon)} \sum_j^{N_0} \left[\frac{I(\varepsilon_i > \varepsilon > \varepsilon_j)}{k\Delta\varepsilon_i\, \Delta\varepsilon_j}\right]_j \tag{88}$$

where $N_0(\varepsilon)$ is the number of points sampled on the surface ε and $I(\varepsilon_i > \varepsilon > \varepsilon_f) = 1$ if a trajectory starts in the energy interval $\varepsilon_i \pm \Delta\varepsilon_i/2$ and ends in $\varepsilon_f \pm \Delta\varepsilon_f/2$, and is zero otherwise. A plot of $R(\varepsilon_i, \varepsilon_f)$ for $O_2 + Ar$ at $kT/D = 0.1$ is shown in Fig. 5. The numbers in the boxes are the mean value of $R(\varepsilon_i, \varepsilon_f)/R_V(0)$ for the box. The reference rate $R_V(0)$ is the barrier rate for the surface

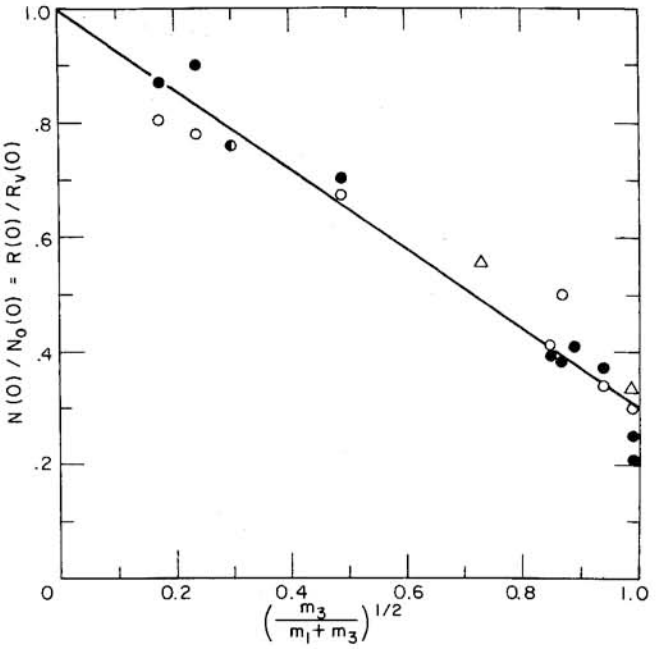

FIG. 3. Fraction of "reacting" trajectories for the surface $\varepsilon = (E - B)/kT = 0$ as a function of the parameter $[m_3/(m_1 + m_3)]^{1/2}$: $kT/D = 0.01$ (○), 0.05 (△), 0.1 (●). The straight line is a "best fit" to the points.

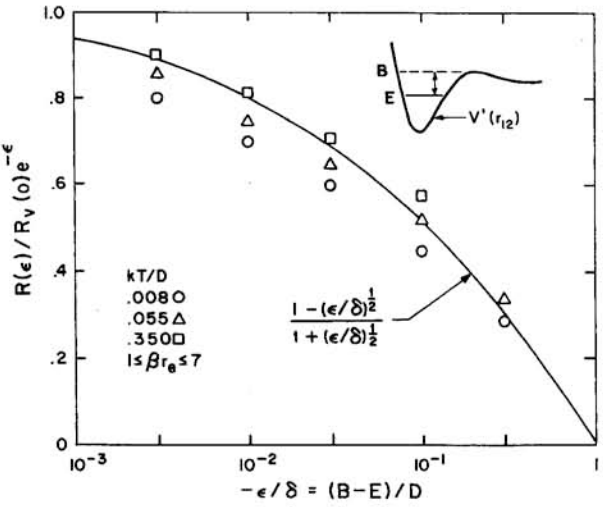

FIG. 4. Calculated values of $G(E) = R_V(\varepsilon)e^{\varepsilon}/R_V(0)$ as a function of energy relative to the top of the rotational barrier for homonuclear molecules interacting with repulsive third bodies at several temperatures. The curve is an empirical fit to the points.

$\varepsilon = 0$. Because of the sampling technique employed, each value of ε used gives data in a quadrant that touches the main diagonal $\varepsilon_i = \varepsilon_f$ at a point $(\varepsilon_i + \varepsilon_f)/2 = \varepsilon$. A sample of 800 trajectories was used for each value of ε. The statistical errors based on the standard deviation range from $\pm 10\%$ for the small boxes touching the main diagonal to $\pm 30\%$ for the large boxes farthest from the main diagonal. The results shown are for $\varepsilon_i > \varepsilon_f$, however, since $R(\varepsilon_i, \varepsilon_f)$ is symmetric in ε_i and ε_f, the results for $\varepsilon_i < \varepsilon_f$ may be obtained by reflection in the main diagonal. It can be seen that in the range investigated $R(\varepsilon_i, \varepsilon_f)$ varies relatively slowly with the mean energy $\bar{\varepsilon} = (\varepsilon_i + \varepsilon_f)/2$ but decreases sharply as the magnitude of the energy transfer $|\Delta| = |\varepsilon_i - \varepsilon_f|$ increases.

To use data of this type in the solution of the master equation (5), it is convenient to represent $R(\varepsilon_i, \varepsilon_f)/R_V(0)$ as a separable kernel in the form

$$R(\varepsilon_i, \varepsilon_f)/R_V(0) = r(\varepsilon_i, \varepsilon_f) = \begin{cases} r_1(\varepsilon_i) r_2(\varepsilon_f); & \varepsilon_i < \varepsilon_f \\ r_1(\varepsilon_f) r_2(\varepsilon_i); & \varepsilon_i > \varepsilon_f \end{cases} \tag{89}$$

A simple three parameter function which has been found to give excellent results is

$$r(\varepsilon_i, \varepsilon_f) = AG(\varepsilon_f) e^{\alpha\varepsilon_f - \beta\varepsilon_i}; \qquad \varepsilon_i \geq \varepsilon_f \tag{90}$$

where A, α, and β are constants and $G(\varepsilon_f)$ is a function which may be arbitrarily specified. The smooth curves in Fig. 5 show a fit of this type and they can be seen to represent the data very well. The function $G(\varepsilon)$ was taken to be

$$G(\varepsilon) = \frac{R_V(\varepsilon) e^{\varepsilon}}{R_V(0)} \approx \frac{[1 - (-\varepsilon/\delta)^{1/2}]}{[1 + (-\varepsilon/\delta)^{1/2}]} \tag{91}$$

and is shown in Fig. 4. The points were computed by Woznick (1965b) and apply to homonuclear molecules interacting with repulsive third bodies. The curve in the figure is a convenient empirical fit to the points. The corresponding data for heteronuclear molecules is not yet available. The constants A, α, and β were obtained by fitting the low-order moments of the energy transfer $\varepsilon_i - \varepsilon_f$ obtained from the numerical data to the corresponding quantities computed for the assumed kernel (90).

To do this we define the moments

$$\begin{aligned} D_n(\varepsilon) &= Ae^{\varepsilon} \int_{-\infty}^{\varepsilon} \int_{\varepsilon}^{\infty} (\varepsilon_i - \varepsilon_f)^{n-1} e^{\alpha\varepsilon_f - \beta\varepsilon_i} \, d\varepsilon_i \, d\varepsilon_f \\ &= Ae^{\varepsilon} \int_0^{\infty} \int_{\varepsilon - \Delta/2}^{\varepsilon + \Delta/2} \Delta^{n-1} e^{-a\Delta - b\bar{\varepsilon}} \, d\bar{\varepsilon} \, d\Delta \\ &= \left(\frac{2A}{b}\right) e^{(1-b)\varepsilon} \int_0^{\infty} \Delta^{n-1} e^{-a\Delta} \sinh\left(\frac{b\Delta}{2}\right) d\Delta \end{aligned} \tag{92}$$

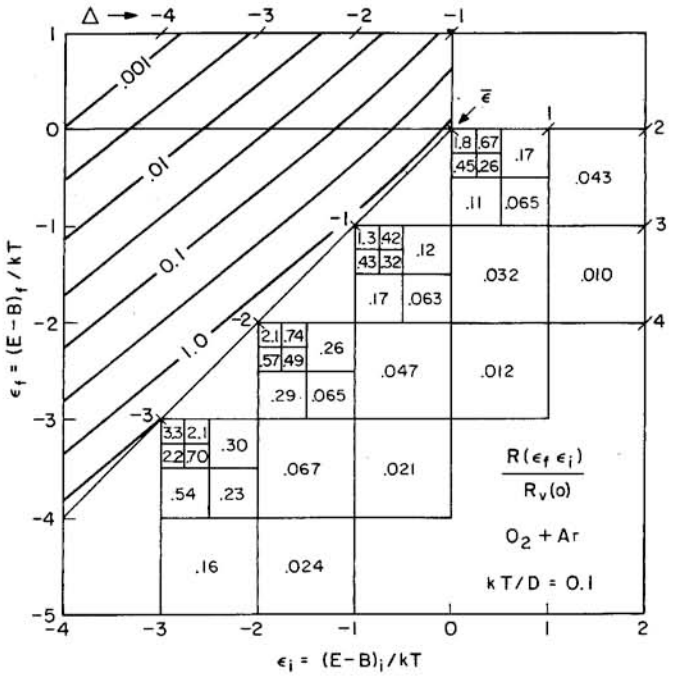

FIG. 5. Differential equilibrium transition rate $R(\varepsilon_i, \varepsilon_f)$ for $O_2 + Ar$ collisions. Numbers in boxes are averages for the box. The smooth curves are a fit of Eq. (90) to the data.

where $\alpha = a - b/2$ and $\beta = a + b/2$. In general, $a \gg b$, and to a good approximation

$$D_n(\varepsilon) \approx An!a^{-n-1}e^{(1-b)\varepsilon} \tag{93}$$

Using (90) we also have

$$D_n(\varepsilon) = e^{\varepsilon} \int_{-\infty}^{\varepsilon} \int_{\varepsilon}^{\infty} (\varepsilon_i - \varepsilon_f)^{n-1} G^{-1}(\varepsilon_f) r(\varepsilon_i, \varepsilon_f)\, d\varepsilon_i\, d\varepsilon_f \tag{94}$$

Evaluating this integral by Monte Carlo methods we obtain

$$D_n(\varepsilon) = \frac{1}{N_0(\varepsilon)} \sum_{j}^{N_0} (\varepsilon_i - \varepsilon_f)_j^{n-1} \left(\frac{G(\varepsilon)}{G(\varepsilon_f)}\right)_j \left(\frac{I(\varepsilon)}{k}\right)_j \tag{95}$$

where $I(\varepsilon) = 1$ if $\varepsilon_i > \varepsilon > \varepsilon_f$, and is zero otherwise.

The quantities $D_n(\varepsilon)$ are very useful for characterizing the transition kernel and are a much more accurate and efficient way of presenting the numerical results than plots of the type shown in Fig. 5. For transition kernels satisfying the condition $[\delta R(\varepsilon_i, \varepsilon_f)/\delta\Delta]_{\bar{\varepsilon}} \gg [\delta R(\varepsilon_i, \varepsilon_f)/\delta\bar{\varepsilon}]_{\Delta}$, they are approximately

related to the "one way" equilibrium crossing rate (19) and moments (34) by the expressions

$$R(\varepsilon)/R_V(\varepsilon) = D_1(\varepsilon) \tag{96}$$

and

$$\frac{\Delta_n(\varepsilon)}{R_V(\varepsilon)} = [1 + (-1)^n]D_n(\varepsilon) + \tfrac{1}{2}[1 - (-1)^n]\frac{dD_{n+1}(\varepsilon)}{d\varepsilon}. \tag{97}$$

Thus they may be used directly to obtain the quantities necessary to solve the equivalent diffusion equation (33).

A summary of the low-order $D_n(\varepsilon)$'s is given in Table IV for the systems for which they are available at the present time. Using this data the constants A/a^2 and b can be determined by plotting

$$\ln D_1(\varepsilon) = \ln(N(\varepsilon)/N_0(\varepsilon)) = (1 - b)\varepsilon + \ln(A/a^2) \tag{98}$$

as a function of ε as shown in Fig. 6. The slopes of the lines give $(1 - b)$ and the intercept at $\varepsilon = 0$ gives A/a^2. The constant a can be determined by

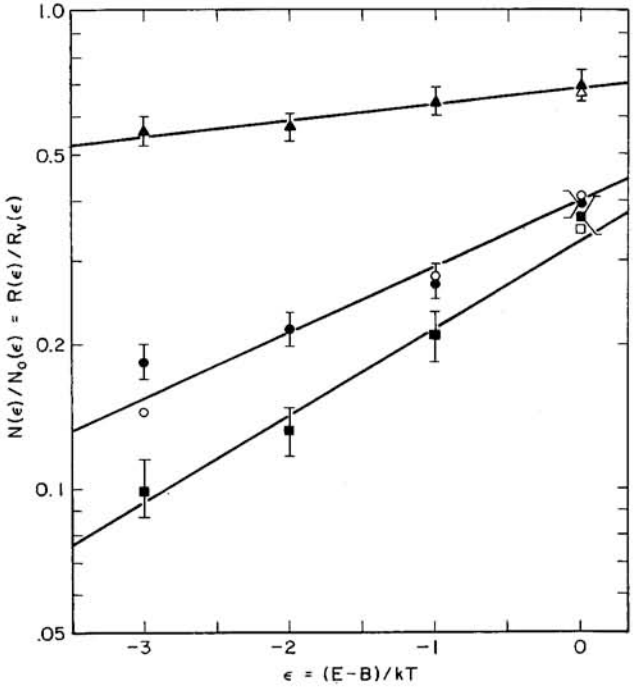

FIG. 6. Fraction of "reacting" trajectories as a function of ε for $I_2 + A$ (triangles), $O_2 + A$ (circles), and $O_2 + Xe$ (squares) at $kT/D = .01$ (closed symbols), and 0.1 (open symbols). The straight lines are a "best fit" to data.

taking the ratio of successive moments. Using the data in Table IV we have formed the combinations D_1/D_0, $2D_1/D_2$, and $(12D_2/D_4)^{1/2}$ which are also shown and each of which gives a value for a. Although there is considerable statistical scatter in these ratios there appears to be no significant dependence on the value of ε. We have therefore averaged the values for various ε's to obtain the results shown in parentheses. Inspection of these results shows that the apparent value of a decreases as the energy transfer increases. Thus, the simple exponential form (90) does not give an exact fit, and the true kernel gives a somewhat higher probability for both small and large energy transfers. Since we anticipate from the diffusion analysis that it is the first and the second moment which are most important for determining the steady state rate constants, we have used the value of a given by the ratio $2D_1/D_2$ to give a "best fit" to the data.

The values of A, a, b, α, and β determined in the manner just described are shown in Table V. It appears that a is essentially independent of the mass ratio m_3/m_1, but is a weakly increasing function of kT/D. On the other hand,

TABLE IV

SUMMARY OF ENERGY TRANSFER MOMENTS

	$\frac{kT}{D}$	ε	$\frac{N}{N_0}$	D_0	D_2	D_4	$\frac{D_0 N_0}{N}$	$\frac{2N}{D_2 N_0}$	$\left(\frac{12\,D_2}{D_4}\right)^{1/2}$
$I_2 + Ar$	0.1	0	.73	3.64	.64	2.78	5.0	2.3	1.7
		−1	.65	1.52	.72	3.23	2.3	1.8	1.6
		−2	.58	2.11	.65	2.82	3.7	1.8	1.7
		−3	.57	1.12	.63	2.30	2.0	1.8	1.8
							(3.3)	(1.9)	(1.7)
$O_2 + Ar$	0.1	0	.42	1.83	.42	2.09	4.3	2.0	1.4
		−1	.27	1.05	.32	2.00	3.9	1.7	1.4
		−2	.22	1.27	.26	1.50	5.9	1.7	1.4
		−3	.18	.65	.20	1.02	3.5	1.9	1.5
							(4.4)	(1.8)	(1.4)
	.01	0	.41	.93	.59	8.02	2.3	1.4	.9
		−1	.28	.77	.53	9.42	2.8	1.1	.8
		−3	.15	1.20	.23	4.35	8.2	1.3	.8
							(4.4)	(1.3)	(.9)
$O_2 + Xe$	0.1	0	.38	2.27	.47	3.90	6.8	1.6	1.2
		−1	.21	.72	.19	.87	3.5	2.1	1.6
		−2	.13	1.01	.10	.48	7.5	2.7	1.6
		−3	.10	.53	.09	.28	5.3	2.2	2.0
							(5.8)	(2.1)	(1.6)
	.01	0	.35	2.00	.47	6.7	(5.6)	(1.5)	(.9)

b is independent of kT/D, but is a weakly decreasing function of increasing mass ratio. Note that $\sqrt{2}/a$ is just the rms energy transfer per collision in units of kT, and b is the parameter which determines the position of the minimum in $r(\varepsilon_i, \varepsilon_f)$ along the main diagonal in Fig. 5. The larger the value of b, the closer the minimum is to the dissociation limit.

TABLE V

CONSTANTS USED TO FIT ASSUMED TRANSITION KERNEL (90) TO DATA

	m_3/m_1	kT/D	A	a	b	α	β
$I_2 + Ar$	.32	0.1	1.2	1.9	.93	1.4	2.0
$O_2 + Ar$	2.5	0.1	1.4	1.8	.71	1.4	2.2
$O_2 + Xe$	8.2	0.1	3.0	2.1	.58	1.8	2.4
$O_2 + Ar$	2.5	.01	.68	1.3	.71	1.0	1.6
$O_2 + Xe$	8.2	.01	1.5	1.5	—	—	—

It is apparent from the results presented in this section that the mechanics of three-body collisions is a good deal simpler than one might have suspected *a priori*. Additional studies are needed particularly for heteronuclear molecules and attracting third bodies. However, even with the correlations developed to date, Shui, Appleton, and Keck (1970a, b), and Shui and Appleton (1971), have shown that it is possible to fit all of the measured rate constants for the dissociation or recombination of homonuclear diatomic molecules in collisions with noble gases. Although in their initial investigations Shui, Appleton, and Keck were unable to fit the rate constant for the heteronuclear molecules HF and HCl, it has since been determined that this was due to the extension of a correlation valid for homonuclear molecules to the heteronuclear case. Recent Monte Carlo studies, some of which are reported here, have resolved this difficulty and there is now good agreement between theory and experiment for the heteronuclear case as well (Shui *et al.*, 1972)

V. Atomic Excitation and Ionization

Monte Carlo studies of atomic excitation and ionization in three-body collisions have been made by Mansbach and Keck (1969) for low temperature thermal electrons, Abrines, Percival, and Valentine (1966) for high energy monochromatic electrons, and Abrines and Percival (1966) for high energy monochromatic protons.

In the work of Abrines *et al.* an impact parameter formulation was used and attention was focused on direct ionization and exchange scattering for

atoms initially in a specified quantum state. The energies of the incident electrons or protons were always greater than the ionization potential and no information about direct scattering was presented. Since thermal excitation and ionization involve primarily direct scattering of electrons with energies less than the ionization potential, these results are not directly applicable to this problem and will not be discussed in detail. In general the Monte Carlo calculations agreed reasonably well with the predictions of previous classical theories. They also agreed with experimental measurements for protons and high energy electrons. For low energy electrons, however, the calculated ionization cross sections were somewhat larger than the measured ones and Abrines *et al.* suggest that this is probably the result of neglecting interference between direct and exchange scattering.

In the work of Mansbach and Keck, the trajectories were sampled on the constant energy surfaces $E_{12}/kT = \varepsilon$, where $E_{12} = p_{12}^2/2m - e^2/r_{12}$, is the energy of the electron in the atom. In the energy range $0.03 \leq kT \leq 1.0$ eV investigated, the most important process was direct excitation by incident electrons with a mean energy substantially less than the ionization energy. Exchange occurred in approximately 15% of the cases but was not separated from the direct process. The most important results of these calculations are summarized in Fig. 7, 8, and 9. Figure 7 shows that within the statistical errors the fraction of trajectories $N(\varepsilon)/N_0(\varepsilon)$ making the transition $\varepsilon_i > \varepsilon > \varepsilon_f$ is independent of temperature for the surface $\varepsilon = -3$. Figure 8 shows that in the range $0.5 \leq \varepsilon_i - \varepsilon_f \leq 6$ the ratio $R(\varepsilon_i, \varepsilon_f)/e^{-\varepsilon_i}$ is substantially

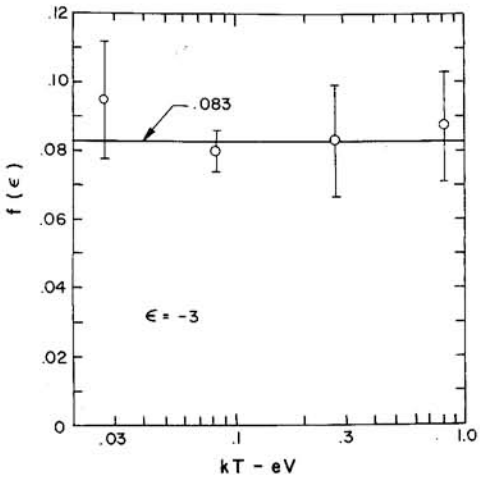

FIG. 7. Fraction of "reacting" trajectories $f(\varepsilon) = N(\varepsilon)/N_0(\varepsilon)$ for $H + e$ collisions as a function of temperature for the surface $\varepsilon = -3$.

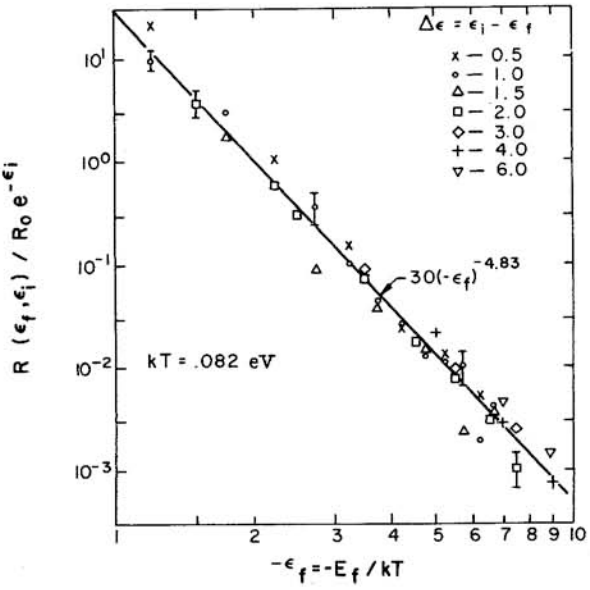

FIG. 8. Plot of $R(\varepsilon_i, \varepsilon_f)e^{\varepsilon_i}$ as a function of ε_f for $H + e$ collisions. Errors shown are typical of points in their neighborhood.

independent of energy transfer and varies as $(-\varepsilon_f)^{-4.83}$ for $kT = .082$ eV. Thus, $R(\varepsilon_i, \varepsilon_f)$ can be fit with the simple separable kernel

$$R(\varepsilon_i, \varepsilon_f) = 30\, R_0\, e^{-\varepsilon_i}(-\varepsilon_f)^{-4.83}; \qquad \varepsilon_i > \varepsilon_f \tag{99}$$

where

$$R_0 = (e^2/kT)^5(kT/m)^{1/2}[H^+]_e\,[e]_e^2 \tag{100}$$

is a characteristic equilibrium three-body recombination rate. This kernel is compared with the numerical results in Fig. 9, which is analogous to Fig. 5 discussed in the preceding section. It can be seen that the fit is quite good.

Unfortunately, the moments $D_n(\varepsilon)$ were not calculated directly in this case but (99) may be used to generate them analytically. The root-mean-square energy transfer per collision obtained in this way is

$$\langle \Delta\varepsilon \rangle_{rms} = \{2[1 \times .050(-\varepsilon_i)^3]/[1 + (-\varepsilon_i/3.83)]\}^{1/2} \tag{101}$$

which is slightly larger than the values obtained for molecular excitation and implies an energy transfer of order $2\,kT$ in the vicinity of the minimum of $R(\varepsilon_i, \varepsilon_f)$ on the main diagonal.

The kernel (99) may also be used to obtain the Maxwell averaged differential cross section for energy transfer defined by

$$d\sigma(\varepsilon_i, \varepsilon_f)/d\varepsilon_f = R(\varepsilon_i, \varepsilon_f)/\bar{c}_e[e]_e[d[H]/d\varepsilon_i]_e \tag{102}$$

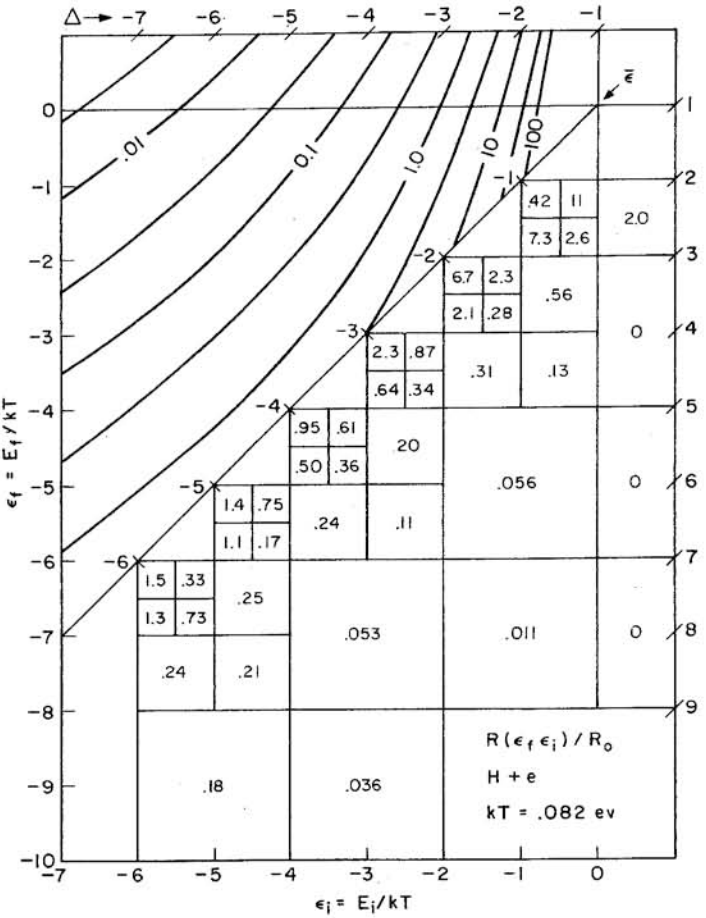

FIG. 9. Differential equilibrium transition rate $R(\varepsilon_i, \varepsilon_f)$ for $H + e$ collisions. Numbers in boxes are averages for the box. The smooth curves are a fit of Eq. (99) to the data.

where $\bar{c}_e = (8\,kT/\pi m)^{1/2}$ is the thermal speed of the electrons and

$$(d[\mathrm{H}]/d\varepsilon)_e = [e]_e[\mathrm{H}]_e\,(\pi/2)^{3/2}(e^2/kT)^3[e^{-\varepsilon}/(-\varepsilon)^{5/2}] \tag{103}$$

is the equilibrium density of atoms per unit ε. Substituting (99) and (103) into (102) we find

$$d\sigma(\varepsilon_i, \varepsilon_f)/d\varepsilon_f = \sigma_T\, 2.3\begin{cases}(-\varepsilon_f)^{-4.83}(-\varepsilon_i)^{2.5}; & \varepsilon_i > \varepsilon \\ (-\varepsilon_i)^{-2.33}e^{-(\varepsilon_f-\varepsilon_i)}; & \varepsilon_f > \varepsilon_i\end{cases}$$

where $\sigma_T = \pi(e^2/kT)^2$ is the Thompson cross section.

It is of some interest to compare the Monte Carlo results with the classical results of Gryzinski (1959, 1965) since the latter have been widely used in collisional-radiative cascade theories of ionization (Bates *et al.*, 1962; Byron *et al.*, 1962; Norcross and Stone, 1968). This is done in Fig. 10 where we have plotted the transition kernel $R(\Delta, \bar{\varepsilon})$ computed from Gryzinski's cross sections along with the Monte Carlo results as a function of Δ for $\bar{\varepsilon} = -3$. It can be seen that for large energy transfers Gryzinski's exact results asymptotically approach the Monte Carlo results. For small energy transfers, however, they are very much larger and diverge as Δ^{-3}. This suggests a serious breakdown of the impact approximation in this range.

In cascade theories the divergence has been eliminated by introducing a cutoff at the level spacing. The reason this has not produced serious errors is probably due to the fact that it is the second moment of the energy transfer which is most important in controlling the transition rates and this only diverges logarithmically.

Mansbach and Keck (1969) have compared their Monte Carlo results with experimental measurements under conditions where radiative processes

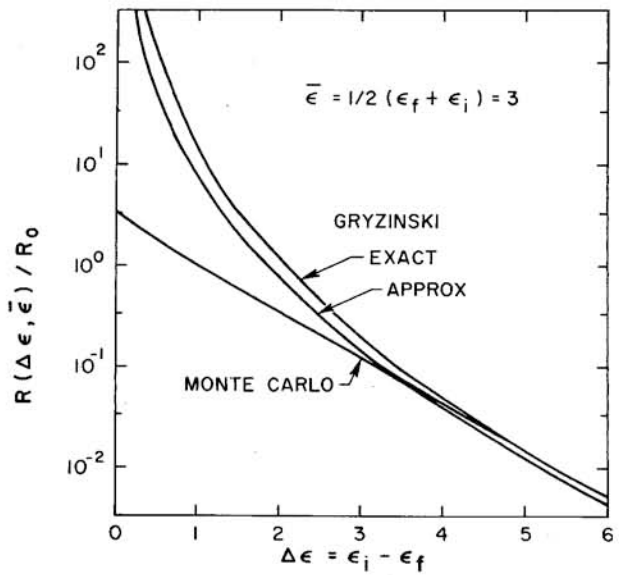

FIG. 10. Comparison of differential equilibrium transition rate obtained by Monte Carlo methods with results computed from Gryzinski's "exact" and "approximate" cross sections obtained by using the impulse approximation. Gryzinski's results which diverge as $(\Delta\varepsilon)^{-3}$ overestimate the probability of small energy transfers by a large factor. This is the result of using the impulse approximation in a region where the collisions are highly adiabatic.

play a minor role. They find good agreement for the steady state distribution function and the temperature dependence of the recombination coefficient. However, the magnitude of the recombination coefficient is about a factor of 2 low. It was suggested that this may be due to the combined effect of radiative cascading at high temperature and dissociative recombination at low degrees of ionization. Both these processes tend to increase the measured rates.

ACKNOWLEDGMENT

The author is indebted to John Appleton and Ven Shui for many helpful discussions and suggestions regarding this work.

REFERENCES

Abrines, R., and Percival, I. C. (1966). *Proc. Phys. Soc. London* **88**, 873.
Abrines, R., Percival, I. C., and Valentine, N. A. (1966). *Proc. Phys. Soc., London* **89**, 515.
Bates, D. R., Kingston, A. E., and McWhirter, R. W. P. (1962). *Proc. Roy. Soc., Ser. A* **267**, 297.
Brau, C. A., Keck, J. C., and Carrier, G. F. (1966). *Phys. Fluids* **9**, 1885.
Bunker, D. L., and Pattengill, M. (1968). *J. Chem. Phys.* **48**, 722.
Byron, S., Stabler, R. C., and Bortz, P. I. (1962). *Phys. Rev. Lett.* **8**, 376.
Gryzinski, M. (1959). *Phys. Rev.* **115**, 374.
Gryzinski, M. (1965). *Phys. Rev. A* **138**, 322.
Hammersley, J. M., and Handscomb, D. C. (1964). "Monte Carlo Methods." Wiley, New York.
Keck, J. (1962). *Discuss. Faraday Soc.* **33**, 173.
Keck, J. C. (1967). *Advan. Chem. Phys.* **13**, 85.
Keck, J., and Carrier, G. (1965). *J. Chem. Phys.* **43**, 2284.
Keck, J., and Kalelkar, A. (1968). *J. Chem. Phys.* **49**, 3211.
Kuntz, P. J., Nemeth, E. M., Polonyi, J. C., and Wong, W. H. (1970). *J. Chem. Phys.* **52**, 4654.
Mansbach, P., and Keck, J. (1969). *Phys. Rev.* **181**, 275.
Meyer, H. A., ed. (1956). "Symposium on Monte Carlo Methods." Wiley, New York.
Mok, M. H., and Polanyi, J. C. (1970). *J. Chem. Phys.* **53**, 4588.
Montroll, E. W., and Shuler, K. E. (1958). *Advan. Chem. Phys.* **1**, 361.
Morokuma, K., and Karplus, M. (1971). *J. Chem. Phys.* **55**, 63.
Norcross, D. W., and Stone, P. M. (1968). *J. Quant. Spectrosc. Radiat. Transfer* **8**, 655.
Shui, V. H., and Appleton, J. P. (1971). *J. Chem. Phys.* **55**, 3126.
Shui, V. H., Appleton, J. P., and Keck, J. C. (1970a). *J. Chem. Phys.* **53**, 2547.
Shui, V. H., Appleton, J. P., and Keck, J. C. (1970b). *Symp. (Int. Combust., Proc.* 13*th*, p. 21.
Shui, V. H., Appleton, J. P., and Keck, J. C. (1972). *J. Chem. Phys.* **56**, 4266.
Wall, F. T., Hiller, L. A., and Mazur, J. (1961). *J. Chem. Phys.* **35**, 1284.
Woznick, B. J. (1965a). Res. Rep. No. 223. AVCO Res. Lab., Everett, Massachusetts.
Woznick, B. J. (1965b). *J. Chem. Phys.* **42**, 1151.